ISSN 1070-3284, Russian Journal of Coordination Chemistry, 2016, Vol. 42, No. 5, pp. 338–344. © Pleiades Publishing, Ltd., 2016.

Two 3D Zinc-Bpe Frameworks Constructed from 2-Carboxyl/Sulfo-Terephthalate: Crystal Structures and Luminescent Properties[1]

Y. Ren[a, b, *], H. Chai[b], M. An[a, b], L. Gao[b], and G. Zhou[b]

[a] *Department of Chemistry, School of Science, Xi'an Jiao Tong University, Xi'an, 710049 P.R. China*

[b] *College of Chemistry and Chemical Engineering, Shaanxi Key Laboratory of Chemical Reaction Engineering, Yan'an University, Yan'an 716000, Shaanxi, P.R. China*

**e-mail: renyixia1@163.com*

Received July 18, 2015

Abstract—Two new zinc(II) complexes with the formulas of [Zn(HTma)(Bpe)] (**I**) and [$Zn_{1.5}$(Stp)(Bpe)(H_2O)$_2$] (**II**), where H_3Tma = 1,2,4-trimellitic acid, Bpe = 1,2-bis(4-pyridyl)ethane, NaH_2Stp = monosodium 2-sulfoterephthalate, have been prepared under hydrothermal conditions. Structural syntheses show complex **I** is a five-fold interpenetrated three-dimensional structure based on the diamond-like networks, however, complex **II** is a Bpe-pillared three-dimensional framework (CIF files CCDC nos. 1404475 (**I**) and 140447 (**II**)). Thermogravimetric analyses show that complex **I** possesses high thermal stability up to 325°C and the dehydrated product of complex **II** also begins to decompose from 357°C. The luminescent properties of the two complexes are investigated in solid state.

DOI: 10.1134/S1070328416050067

INTRODUCTION

Extensive researches about the design and construction of metal-organic frameworks (MOFs) have been reported in recent years [1–3]. These researches result in an extensive class of crystalline materials with charming structural features, such as multi-fold interpenetration, helix or entanglement, polynuclear metallic cluster and so on [4–7]. Furthermore, the MOFs also exhibit high stability, tunable porosity, luminescence, magnetic, catalysis [8, 9]. As one important class of MOFs materials, the Zn-MOFs have been widely investigated in the past two decade years for the more foreseeable coordination polyhedron of zinc ion compared with other metal MOFs [10–12]. The famous MOF-5 was an exceptionally stable and highly porous Zn-MOFs material reported in [13]. And great deals of organic ligands are used in the construction of Zn-MOFs, especially the multi-carboxylic acids for the versatile coordination fashions of the carboxyl group [14–16]. Terephthalate ligand possesses two carboxyl groups in 1- and 4-site of phenyl ring and is apt to form the bridging coordinated with metal ions as a straight linker, for example MOF-5. If the 2-site H atom is substituted by other functional groups, for instance carboxyl, sulfonate, hydroxyl, nitro-groups or halogen, the coordination modes of the organic ligand will be different and the structural features of Zn-MOFs will be changed. So we try to prepare new Zn-MOFs based on 1,2,4-trimellitic acid (H_3Tma) and 2-sulfoterephthalate ligand (H_2Stp^-) with 1,2-bis(4-pyridyl)ethane (Bpe). Fortunately, we obtained two new Zn-Bpe frameworks with $HTma^{2-}$and Stp^{3-} ligands. The two complexes display the different three-dimensional structures as described in this paper and their thermal stabilities and luminescent properties in solid state are studied. The coordination fashion of $HTma^{2-}$ (a) and Stp^{3-} (b) ligands in **I** and **II** are below:

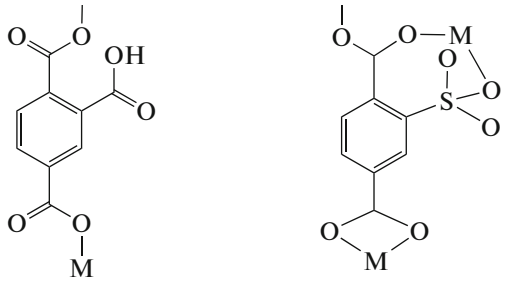

(a) $\eta^1:\eta^1:\mu_2$ (b) $\eta^1:\eta^1:\eta^1:\eta^1:\eta^1:\mu_3$

Scheme.

EXPERIMENTAL

Materials and measurements. All chemicals were commercially available and used as received without

[1] The article is published in the original.

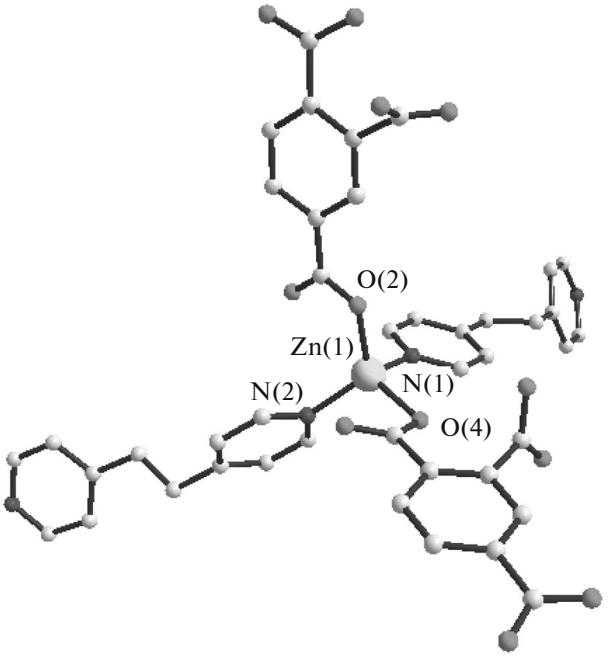

Fig. 1. The coordination environment of Zn^{2+} ion in **I**. The hydrogen atoms are omitted for clarity.

further purification. Elemental analyses (CHN) were performed using an Vario EL elemental analyzer. FT-IR spectra were recorded from KBr pellets in the range of 4000–400 cm^{-1} on a Nicolet Avatar 360 FT-IR spectrometer. Thermogravimetric (TG) curves were measured on a Mettler (USA) at a heating rate of 10°C/min from room temperature to 900°C in nitrogen atmosphere. Fluorescence measurements were carried out with a SHIMADZU RT5301PC spectrofluorophotometer.

Synthesis of [Zn(HTma)(Bpe)] (I). A mixture of $Zn(OAc)_2$ (0.013 g, 0.05 mmol), H_3Tma (0.016 g, 0.05 mmol) and Bpe (0.012 g, 0.05 mmol) was added to a 3 mL aqueous solution. The mixture was stirred for 5 min and was placed in a 23 mL Teflon-lined stainless steel autoclave and heated at 160°C for 72 h. The autoclave was cooled over a period of 16 h in air. The colorless stick-like crystals of **I** were collected by filtration, washed with ethanol, and dried in air (the yield was 58% based on Zn).

For $C_{21}H_{16}N_2O_6Zn$

anal. calcd., %:	C, 55.10;	H, 3.52;	N, 6.12.
Found, %:	C, 54.99;	H, 3.15;	N, 6.04.

IR (ν, cm^{-1}): 3447 m, 1734 s, 1618 s, 1375 s, 1238 m, 1151 m, 1154 m, 1070 m, 1037 m, 841 m, 774 m, 648 m.

Synthesis of $[Zn_{1.5}(Stp)(Bpe)(H_2O)_2]$ (II). A mixture of $Zn(OAc)_2$ (0.013 g, 0.05 mmol), NaH_2Stp (0.026 g, 0.1 mmol) and Bpe (0.018 g, 0.1 mmol) was added to a 3 mL aqueous solution. The mixture was stirred for 5 min and was placed in a 23 mL Teflon-lined stainless steel autoclave and heated at 140°C for 72 h. The autoclave was cooled over a period of 16 h in air. The colorless lath-like crystals of II were collected by filtration, washed with ethanol, and dried in air (the yield was 43% based on Zn).

For $C_{20}H_{19}N_2O_9SZn_{1.5}$

anal. calcd., %:	C, 42.78;	H, 3.41;	N, 4.99.
Found, %:	C, 42.39;	H, 3.22;	N, 4.67.

IR (ν, cm^{-1}): 3439 w, 1615 v.s, 1575 s, 1354 s, 1160 m, 1067 m, 1022 m, 830 w, 774 w, 624 w.

X-ray structure determination. X-ray single-crystal diffraction data of I and II were collected on a Bruker SMART APEX CCD diffractometer with graphite monochromatic MoK_α radiation (λ = 0.71073 Å). Absorption corrections were applied by using the multi-scan program SADABS [17]. The structures were solved using direct methods and refined with a full-matrix least-squares technique with the SHELXTL program package [18, 19]. Metal atoms in each complex were located from the *E*-maps and other non-hydrogen atoms were located in successive difference Fourier syntheses and refined with anisotropic thermal parameters on F^2. The hydrogen atoms were generated geometrically. Data collection and structural refinement parameters of the two complexes are given in Table 1 and selected bond distances are given in Table 2.

Supplementary material for structures has been deposited with the Cambridge Crystallographic Data Centre (CCDC nos. 1404475 (**I**) and 140447 (**II**); deposit@ccdc.cam.ac.uk or http://www.ccdc.cam.ac.uk).

RESULTS AND DISCUSSION

Single-crystal X-ray diffraction analysis of **I** reveals a five-fold interpenetrated diamond-like three-dimensional structure in which the asymmetric unit consists of one Zn^{2+} ion, one $HTma^{2-}$ anion and one Bpe molecule. As shown in Fig. 1, the Zn^{2+} ion lies in a four-coordinated tetrahedral environment with two oxygen atoms (O(2) and O(4)) from two Tma^{3-} anions and two nitrogen atoms (N(1) and N(2)) from two Bpe ligands. The Zn–O bond lengths are 1.994(3) and 1.979(3) Å, and Zn–N bond lengths are 2.026(4) and 2.054(4) Å. The O/N–Zn–O/N angles are in the range of 101.83(16)°–120.92(15)°.

Two adjacent Zn^{2+} ions are linked by Bpe ligands into a bigger left-handed helical chain along *z* axis as shown in Fig. 2. Around the chain, there are four smaller left-handed helical chains based on the $HTma^{2-}$ ligands in μ_2-η_1:η_1 mode coordinated to two adjacent Zn^{2+} ions (Scheme, a). Each bigger helix is

Table 1. Crystal data and structure refinements for **I** and **II**

Parameter	Value	
	I	**II**
Fw	457.73	561.49
T, K	296(2)	293(2)
Crystal system	Tetragonal	Monoclinic
Space group	$P4_3$	$P2_1/c$
a, Å	8.9064(10)	9.2310(15)
b, Å	8.9064(10)	18.5410(3)
c, Å	26.267(6)	15.1348(18)
β, deg	90	122.187
V, Å ^{3}	2.0836(6)	2.1922(6)
Z	4	4
ρ_{calcd}, g cm^{-3}	1.459	1.701
μ, mm^{-1}	1.218	1.806
Limiting indices *hkl*	$-11 \leqslant h \leqslant 11$	$-11 \leqslant h \leqslant 10$
	$-7 \leqslant k \leqslant 11$	$-22 \leqslant k \leqslant 19$
	$-34 \leqslant l \leqslant 34$	$-18 \leqslant l \leqslant 18$
Reflections collected/unique	12969/4906	11315/4069
R_{int}	0.0644	0.0135
Refinement parameter	272	316
GOOF	1.015	1.064
R_1 ($I > 2\sigma(I)$)	0.0578	0.0216
wR_2 (all data)	0.0879	0.0590
Largest diff. peak/hole, *e* Å^{-3}	0.367/−0.303	0.350/−0.330

surrounded by four smaller helixes with the knots of Zn^{2+} ions, so as each smaller helix. According to the arrangement, a network is formed from all left-handed helical chains (Fig. 3). The network possesses a big vacuum which is convenient for storing the lattice or template molecules or forming the interpenetrated structures. In **I**, five such networks are interpenetrated each other into five-fold interpenetrated structures as shown in Fig. 4.

In complex **II**, there are two crystallographically independent Zn^{2+} ions in six-coordinated octahedral geometry. As shown in Fig. 5a, Zn(1) ion is coordinated to three carboxyl O atoms (O(1), O(3*A*) and O(4*A*)) from two Stp ligands, one N atoms (N(1)) from one Bpe ligand, and two O atoms (O(8) and O(9)) from two water molecules. While for Zn(2) ion, there are four O atoms (O(2), O(2*B*), O(5) and O(5*B*)) from the carboxyl and sulfonate groups of two Stp ligands, two N atoms (N(2*C*) and N(2*D*)) from two Bpe ligands, and no water molecules participating in coordinating (Fig. 5b). The Zn–O bond lengths range from 2.003(1) to 2.184(2) Å, and Zn–N bond length are from 2.067(2) to 2.114(2) Å. The O/N–Zn–O/N angles are in the range of 81.36(6)°–180.0(9)°.

The Stp^{3-} ligand adopts a $\eta^1{:}\eta^1{:}\eta^1{:}\eta^1{:}\eta^1{:}\mu_3$ fashion (Scheme, b) joining three Zn^{2+} ions into two-dimensional network shown in Fig. 6. As a based unit of the network, the six-number-ring consists of four Stp^{3-} ligands and six Zn^{2+} ions. In the network, each Zn^{2+} ion is two-connected node linking two Stp^{3-} ligands and each Stp^{3-} ligand is three-connected linking three

Table 2. Selected bond lengths (Å) for **I** and **II***

Bond	*d*, Å	Bond	*d*, Å
I			
Zn(1)–N(1)	2.054(4)	Zn(1)–O(2)	1.944(3)
Zn(1)–N(2)	2.026(4)	Zn(1)–O(4)	1.979(3)
II			
Zn(1)–N(1)	2.0667(7)	Zn(1)–O(9)	2.1836(15)
Zn(1)–O(4)$^{\#1}$	2.0026(13)	Zn(2)–O(2)	2.1008(13)
Zn(1)–O(8)	2.0562(15)	Zn(2)–N(2)$^{\#2}$	2.1135(15)
Zn(1)–O(1)	2.1060(13)	Zn(2)–O(5)	2.1658(12)

* Symmetry codes for **II:** $^{\#1}$ $-1 + x$, $-0.5 - y$, $-0.5 + z$; $^{\#2}$ $2 - x$, $-0.5 + y$, $0.5 - z$.

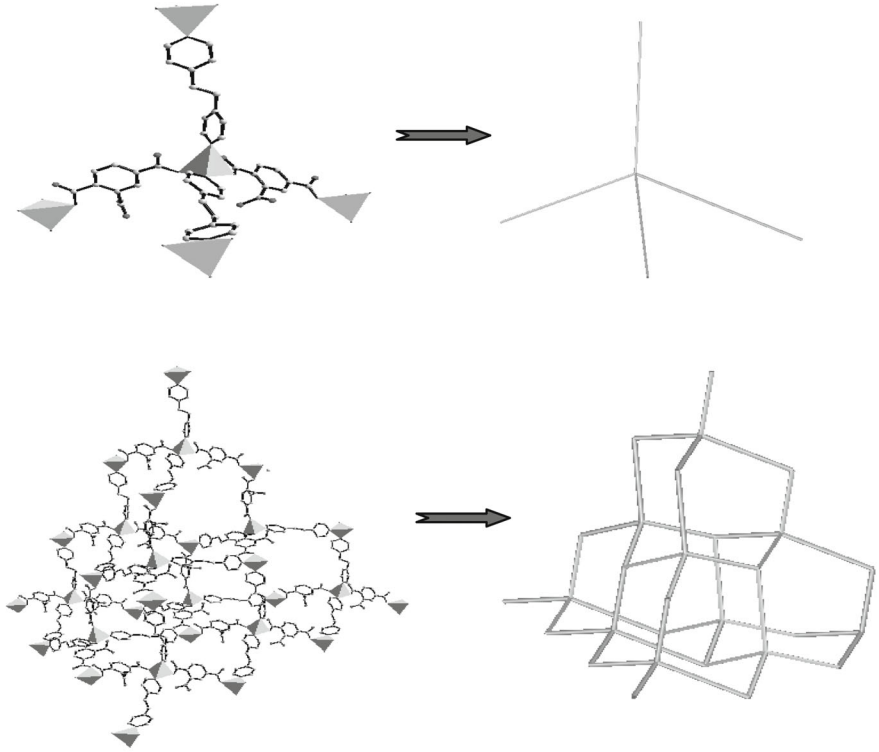

Fig. 2. The diamond-like network in **I**.

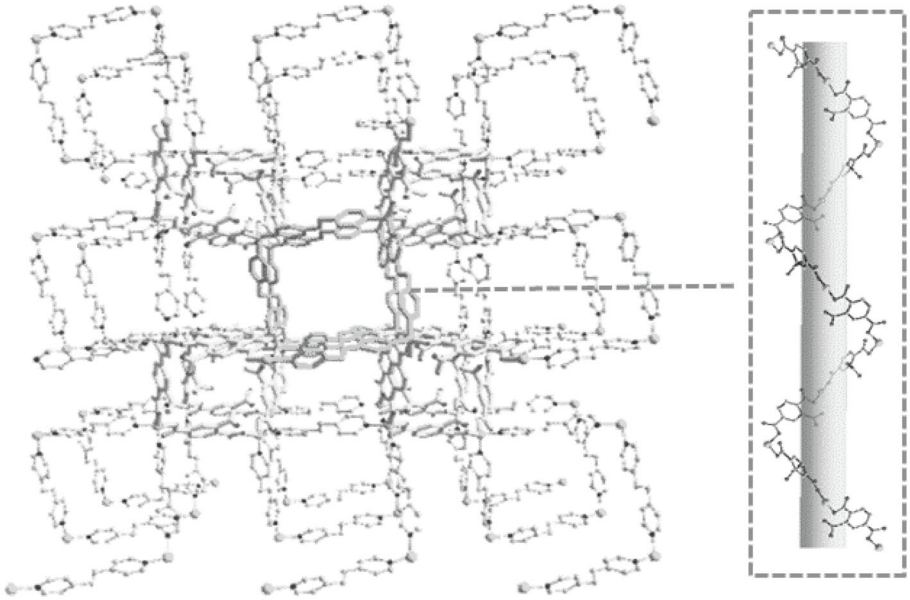

Fig. 3. THE left-handed helical chains existing in complex **I**.

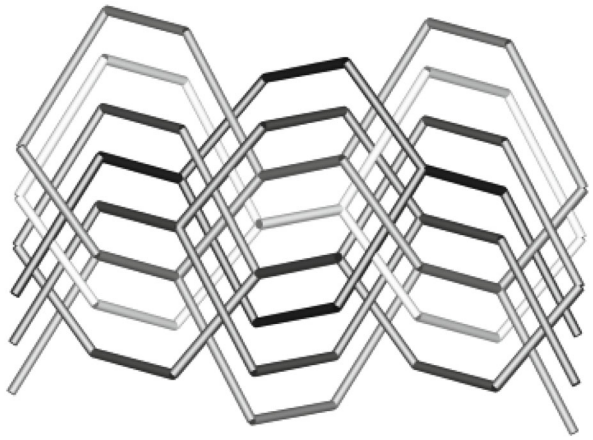

Fig. 4. The five-fold interpenetrated structures in **I**.

Zn^{2+} ions. One Bpe ligand links two Zn^{2+} ions (Zn(1) and Zn(2)) from two networks as pillared units into three-dimensional framework (Fig. 7).

Two three-dimensional Zn-Bpe frameworks with H_3Tma/H_3Stp ligands were prepared under hydrothermal condition. The two carboxylic acids are similar except for 2-site substituting group, however, complexes **I** and **II** exhibit completely different structural features as described above. At first, the coordination environments of Zn^{2+} ions are different: the Zn^{2+} ion in complex **I** is four-coordinated tetrahedral geometry, but for complex **II**, two zinc ions lie in five- and six-coordinated environments. Secondly, the coordination modes of two carboxylic acids (H_3Tma/H_3Stp) are different. 1,2,4-Trimellitic acid adopts a $\eta^1:\eta^1:\mu_2$ fashion in complex **I** linking two zinc ions and 2-site carboxyl group is not deprotonated. While 2-sulfoterephthalate ligand acts as a multidentate linker in a $\eta^1:\eta^1:\eta^1:\eta^1:\eta^1:\mu_3$ mode joining three zinc ions and 2-

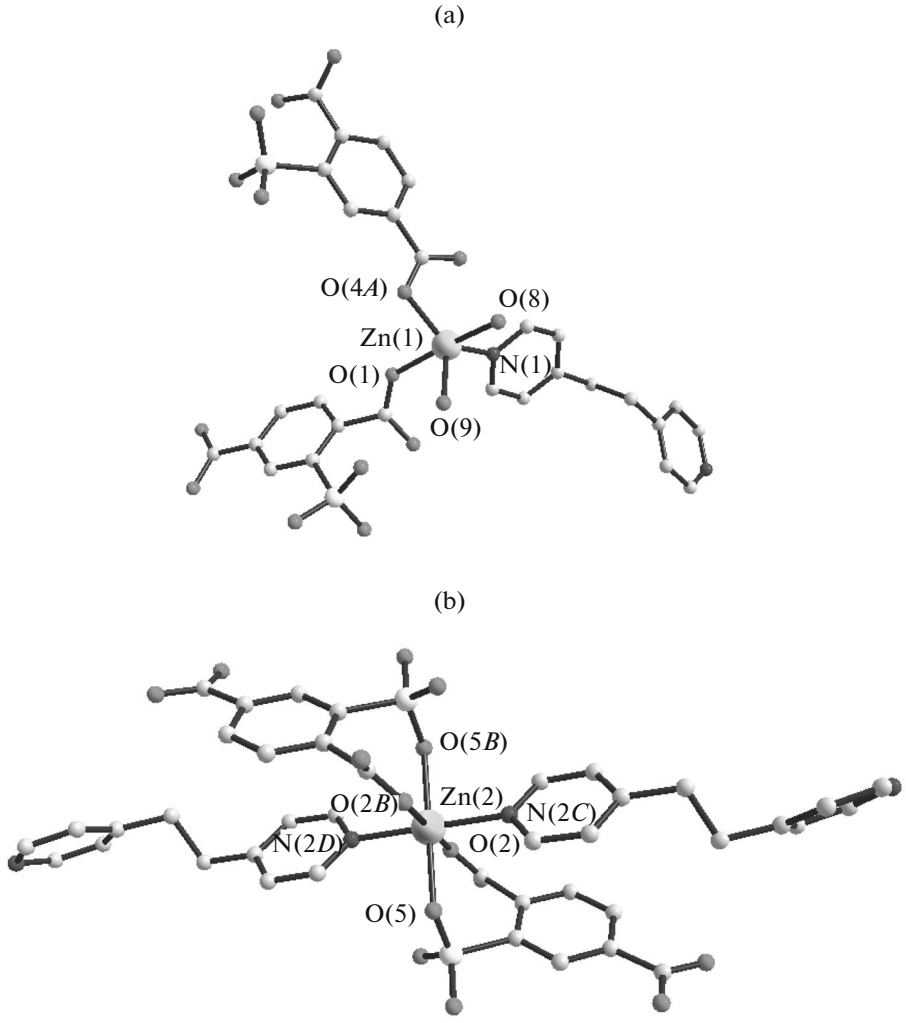

Fig. 5. The coordination environment of Zn(1) (a) and Zn(2) (b) ions in **II**. The hydrogen atoms are omitted for clarity. Symmetry codes: (*A*) $-1 + x, -0.5 - y, -0.5 + z$; (*B*) $2 - x, -y, 1 - z$; (*C*) $2 - x, -0.5 + y, 0.5 - z$; (*D*) $x, 0.5 - y, 0.5 + z$.

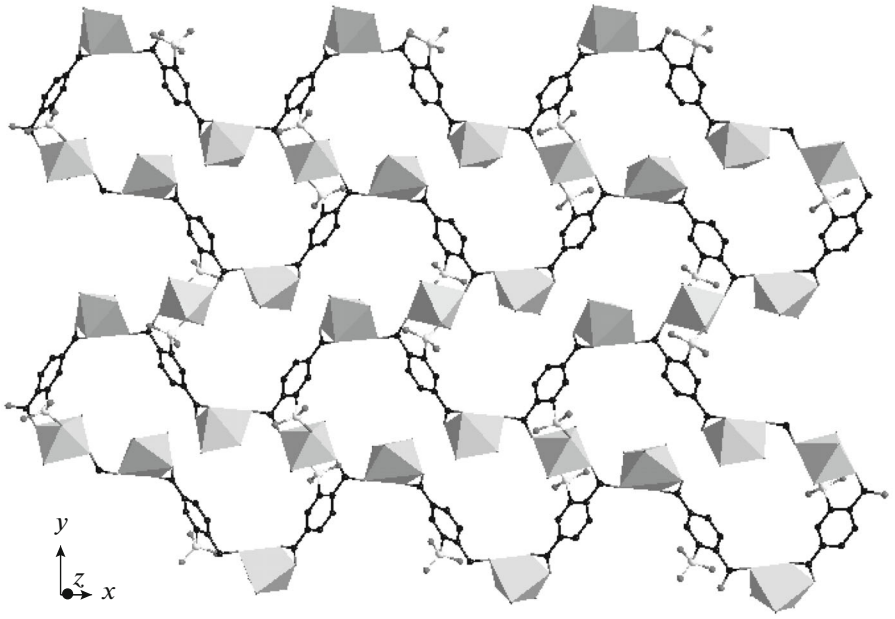

Fig. 6. The 2D network based on Zn^{2+} ions and Stp^{3-} ligands.

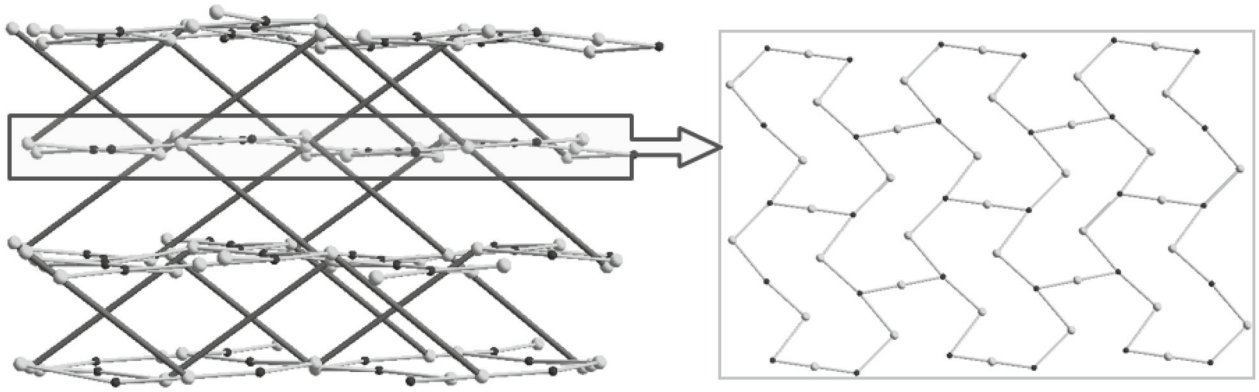

Fig. 7. The Bpe-pillared three-dimensional framework based 2D networks.

site sulfonate group is deprotonated. Finally, the three-dimensional frameworks are distinct. Complex **I** a five-fold interpenetrated three-dimensional structure based on the diamond-like networks, however, complex **II** is a Bpe-pillared three-dimensional framework.

Thermogravimetric (TG) analyses were performed on **I** and **II** in nitrogen atmosphere from 30 to 900°C. For complex **I**, its TG curve shows one step of weight loss from 325 to 576°C, which means the skeleton collapse of the framework beginning from 325°C and the complex possesses higher thermal stability. For **II**, the thermal decomposition procedure can be divided into three steps: the first one from 112 to 163°C with the loss weight ratio is 2.72%, which could be corresponded to the loss of one water molecule (calcd. 3.21%); the second weight loss is 2.84% from 170 to 206°C due to the other water molecule leaving (calcd. 3.21%); the final step begins from 357 to 890°C with the residue ratio is 21.37%, which can be attributed to the decomposition of 3D framework into ZnO (calcd. 21.75% based on 1.5 ZnO). The high thermal ability of complex **I** can be ascribed to its diamond-like structure without lattice and coordinated water molecules, and the dehydrated product of complex **II** also possesses high thermal ability up to 357°C, which is accorded with the results of structural analyses.

The fluorescence spectra of complexes **I** and **II** were determined in solid state at room temperature. The emission spectra of these complexes are different. Complex **I** exhibits one broad band with the maximum emission peaks centered at 440 nm (λ_{ex} = 335 nm), which can be ascribed to the intraligand π–π* emission of Bpe ligand (459 nm) and there are no emission peak for the free H_3Tma ligand in solid state. However, for complex **II**, there are two emission peaks at 457 and 493 nm (λ_{ex} = 387 nm), which is attributed to the intraligand π–π* emission of the two ligands: Stp^{3-} and Bpe, based on the comparison of the location and profile of the emission bands of Na_3Stp (421 nm) and Bpe (459 nm) [20, 21].

ACKNOWLEDGMENTS

This work was supported by the the Natural Scientific Research Foundation of China (no. 21573189) and the Postdoctoral Science Foundation of China (no. 2014M562403).

REFERENCES

1. Jena, H.S., Adhikary, A., and Konar, S., *Inorg. Chem.*, 2014, vol. 53, p. 3926.
2. Ren, Y.X., Zheng, X.J., Li, L.C., et al., *Inorg. Chem.*, 2014, vol. 53, p. 12234.
3. Qian, Yan-Tao, Peng, Ye-Dong, and Zhang, Wen-Wei, *Chin. J. Inorg. Chem.*, 2015, vol. 31, no. 5, p. 857.
4. Zeng, M.H., Tan, Y.X., He, Y.P., et al., *Inorg. Chem.*, 2013, vol. 52, p. 2353.
5. Li, D.S., Wu, Y.P., Zhao, J., et al., *Coord. Chem. Rev.*, 2014, vol. 261, p. 1.
6. Sang, R.L. and Xu, L., *Chem. Commun.*, 2013, vol. 49, p. 8344.
7. Ren, Y.X., Ma, H.Y., Fu, F., et al., *J. Inorg. Organomet. Polym.*, 2013, vol. 23, p. 646.
8. Li, S.M., Zheng, X.J., Yuan, D.Q., et al., *Inorg. Chem.*, 2012, vol. 51, p. 120.
9. Wei, N., Zhang, M.Y., Zhang, X.N., et al., *Cryst. Growth Des.*, 2014, vol. 14, p. 3002.
10. Maret, W.G. and Li, Y., *Chem. Rev.*, 2009, vol. 109, no. 10, p. 4682.
11. Fei, H.H., Han, C.S., Robins, J.C., and Oliver, S.R.J., *Chem. Mater.*, 2013, vol. 25, no. 5, p. 647.
12. He, Y.P., Tan, Y.X., and Zhang, J., *Cryst. Growth Des.*, 2013, vol. 13, no. 1, p. 6.
13. Li, H., Eddaoudi, M., O'Keeffe, M., and Yaghi, O.M., *Nature*, 1999, vol. 402, p. 276.
14. Li, Y.W., Ma, H., Chen, Y.Q., et al., *Cryst. Growth Des.*, 2012, vol. 12, no. 1, p. 189.
15. Guo, Z.G., Cao, R., Wang, X., et al., *J. Am. Chem. Soc.*, 2009, vol. 131, no. 20, p. 6894.
16. Ren, Y.X., Xiao, S.S., Zheng, X.J., et al., *Dalton Trans.*, 2012, vol. 41, p. 2639.
17. Sheldrick, G.M., *SADABS, Program for Empirical Absorption Correction of Area Detector Data*, Göttingen: Univ. of Göttingen, 1996.
18. Sheldrick, G.M., *SHELXL-97 and SHELXTL, Software Reference Manual, Version 5.1*, Madison: Bruker AXS Inc., 1997.
19. *SAINT, Area Detector Control and Integration Software*, Madison (WI, USA): Siemens Analytiacl X-ray Instruments Inc., 1996.
20. Ren, Yi-Xia, Tang, Long, Wu, Yu-Fei, et al., *Chin. J. Inorg. Chem.*, 2012, vol. 28, no. 8, p. 1729.
21. Allendorf, M.D., Bauer, C.A., Bhakta, R.K., and Houk, R.J.T., *Chem. Soc. Rev.*, 2009, vol. 38, p. 1330.